# Global cool ng n t ated stony deserts n central Austral a 2–4 Ma, dated by cosmogen c $^{21}$Ne-$^{10}$Be

Toshiyuki Fujioka*
John Chappell
Masahiko Honda
Igor Yatsevich
Research School of Earth Sciences, Australian National University, Canberra, ACT 0200, Australia
Keith Fifield
Research School of Physical Sciences and Engineering, Australian National University, Canberra, ACT 0200, Australia
Derek Fabel†
Research School of Earth Sciences, Australian National University, Canberra, ACT 0200, Australia

**ABSTRACT**

**Stony deserts are durable indicators of aridity but until now have not been directly dated. Using $^{21}$Ne and $^{10}$Be produced in surface rocks by cosmic rays, we show that Australian stony deserts formed 2–4 Ma, at the time when global cooling initiated the Quaternary ice ages and intensified aridity-induced major landscape changes in central Australia. This is the first direct determination of stony desert ages, using a new method for determining cosmogenic $^{21}$Ne in the presence of various neon components from other sources.**

**Keywords:** late Cenozoic, stony deserts, silcrete, exposure age, cosmogenic Ne/Be.

## INTRODUCTION

Australia today is the driest inhabited continent, but was wetter in the past; plant fossils show that forest covered central Australia until 25–30 Ma (Hill, 1994; White, 1994). Northward continental drift after separation 55 Ma from Antarctica would have led to drying as Australia entered subtropical desert latitudes, but other factors also affected the climate, including Miocene growth of the Antarctic ice sheet, intensified zonality, and development of the Sub-Antarctic oceanic convergence (Bowler, 1982; Hill, 1994; White, 1994; Benbow et al., 1995a). Alkaline lakes developed as conditions became drier in the Miocene. Wetter conditions apparently returned in the Pliocene, before onset of Pleistocene aridity (Benbow et al., 1995a; Simon-Coicon et al., 1996), but chronology and landscape conditions are sketchy.

Present concern about global warming opens the question of whether warming or cooling induced aridity in the past. For example, major droughts occurred in North America in the Medieval Warm Period (Cook et al., 2004). In contrast, aridity intensified in China and other regions, including Australia, during glacial cold periods, evidenced by loess deposits (Ding et al., 2002) and wind-blown dust in marine sediments (Hesse, 1994). Salt-lake sediments indicate that central Australia has been arid for at least the past 0.8–1.1 m.y. (English et al., 2001), but in general the timing and stages of transformation to arid landscapes in Australia are uncertain.

Some arid landforms such as desert sand dunes are prone to reworking and early deposits tend to be obliterated. Thus, only late Pleistocene phases of sand dune activity in Australia have been dated (Nanson et al., 1995; Wasson, 1983). In contrast, stony desert surfaces endure as landscape features. Typically composed of a single layer of varnished stones, known in Australia as gibber (Mabbutt, 1977; Callen and Benbow, 1995), stony desert covers ~10% of the continent. Much of the gibber is derived from silcrete, a resistant rock formed by pedogenic or groundwater silicification of sediment and rock (Thiry and Milnes, 1991; Benbow et al., 1995b; Simon-Coicon et al., 1996). Gibber occurs locally as lag deposit on exposed silcrete pavement, but more widely overlies alluvium or floats on stone-free clayey eolian silt (Mabbutt, 1977). Landscape hydrology is transformed when gibber develops at the expense of soil: runoff from gibber is high (Callen and Benbow, 1995) and vegetation becomes sparse. Once formed, the stony monolayer persists at the ground surface.

To determine when stony desert began to form, we measured exposure ages from gibber-mantled tableland in northern South Australia (Fig. 1). Weathered, near-horizontal Cretaceous and lower Tertiary sediments dominate the region. Saprolite beneath the tableland surface is overprinted by successive weathering regimes: Eocene kaolinization, Oligocene pedogenic silcrete, Miocene bleaching, and Pliocene groundwater silcrete (Thiry and Milnes, 1991; Cook et al., 2004). Exposure ages were determined from gibbers at contrasting sites, including gibbers on a tableland composed of coarse columnar pedogenic silcrete that formed 35–55 Ma (the Cordillo Silcrete; Benbow et al. 1995b; Alley et al., 1996) (Fig. 1, location A; Fig. 2A) and gibbers on an inactive fan below a narrow valley incised into the silcrete tableland (Fig. 2A). The fan gibbers include a component from the tableland, but most appear to have originated as silcrete clasts derived from rocky slopes and low erosion scarps around the upper valley. The fan passes into gibber-mantled lowlands studded with silcrete-capped mesas (Fig. 1). Dissection of the tableland was associated with broad tectonic warping (Benbow et al., 1995b). The third sample, from a second tableland site (Fig. 1, location B), is from a pavement of silcrete gibbers overlying 0.5 m of eolian silt on silcrete-free saprolite (Fig. 2B): the pavement is inferred to be relict from pedogenic silcrete that has been lost to erosion around location B.

Each sample comprised ~20 silcrete clasts, each 4–8 cm in diameter. We assume that soil of unknown depth buried the silcrete before the development of stony desert (Fig. 2C), and that the gibbers have remained at the surface since their parent silcrete was exposed.

*Corresponding author: toshiyuki.fujioka@anu.edu.au.
†Current address: Department of Geographical and Earth Sciences, University of Glasgow, Glasgow G12 8QQ, UK.

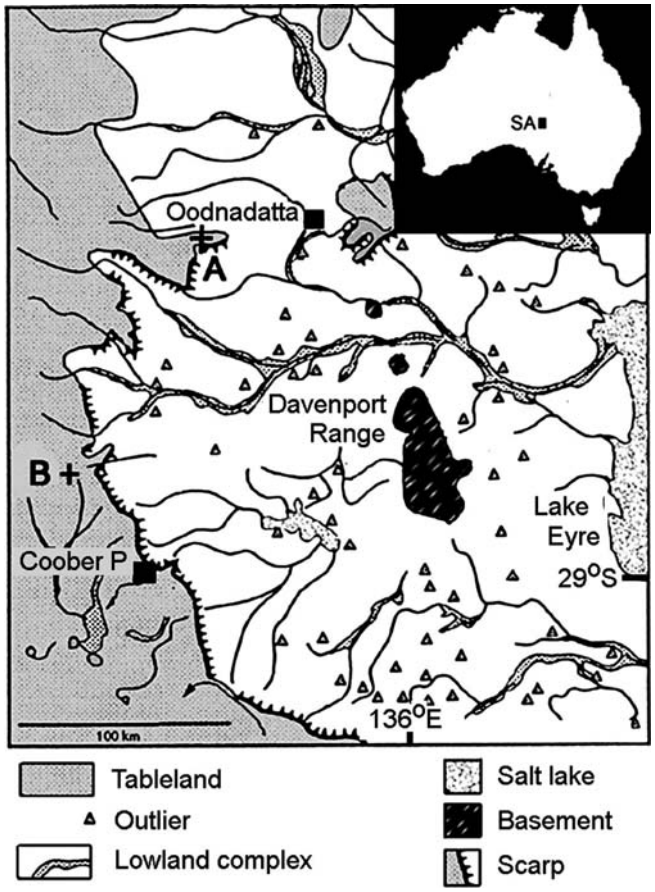


**Figure 1. Stony desert region, northern South Australia (after Simon-Coicon et al., 1996); A and B indicate sampling areas (see Fig. 2 for details). Inset shows location in Australia.**

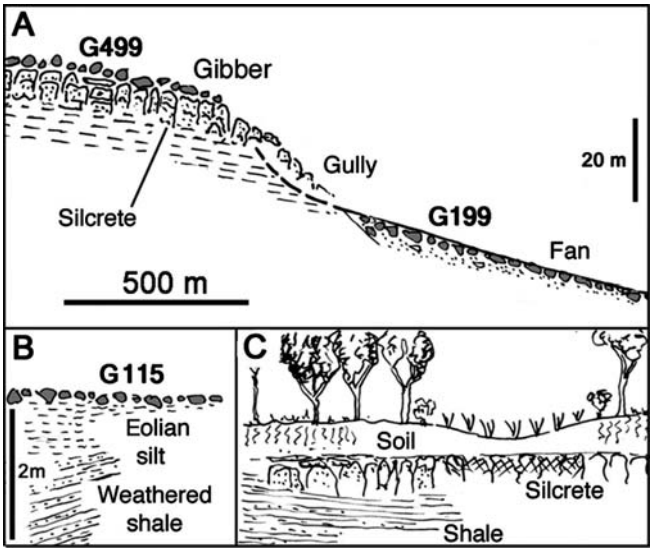


**Figure 2. A and B: Field characteristics of gibber sample sites (locations in Fig. 1). C: Landscape in which silcrete formed (based on Callen and Benbow, 1995; Simon-Coicon et al., 1996; Thiry and Milnes, 1991).**

## EXPERIMENTAL AND ANALYTICAL METHODS

We measured in situ cosmogenic $^{10}$Be and $^{21}$Ne to assess exposure histories. Although $^{10}$Be is widely used in exposure-age dating (Lal, 1991; Gosse and Phillips, 2001), its half-life of $1.5 \times 10^6$ yr limits its range. Cosmogenic $^{21}$Ne is a stable nuclide and potentially extends the exposure dating range. Following standard methods (Kohl and Nishiizumi, 1992), the samples were reduced to ultrapure quartz. $^{10}$Be was measured by accelerator mass spectrometry (AMS) at the Australian National University Heavy Ion Facility (Fifield, 1999), and cosmogenic $^{21}$Ne was determined by noble-gas mass spectrometry (Honda et al., 1993).

### Correction of Interference Neon for Cosmogenic Neon in Silcrete

There are four sources of $^{21}$Ne: cosmogenic, in situ nucleogenic from internal U and Th (Yatsevich and Honda, 1997), trapped crustal nucleogenic (Kennedy et al., 1990), and trapped atmospheric. Meaningful results have been obtained where nucleogenic components were small (Niedermann et al., 1994; Hetzel et al., 2002), but these components are significant in our samples and we used a new method to determine cosmogenic $^{21}$Ne. After mass-spectrometric determination of the relevant isotopes, atmospheric $^{21}$Ne is assessed using: $^{21}Ne_{excess} = {}^{20}Ne_{observed} \times [(^{21}Ne/^{20}Ne)_{observed} - (^{21}Ne/^{20}Ne)_{atmospheric}]$: $^{21}Ne_{excess}$ is a mixture of in situ and crustal nucleogenic and cosmogenic components. In situ nucleogenic $^{21}$Ne produced by the nuclear reaction $^{18}O(\alpha, n)^{21}Ne$, where $\alpha$ particles are provided from a decay of U and Th within the quartz, is calculated with the algorithm of Yatsevich and Honda (1997), using sample U and Th contents (Table 1) and the silcrete formation age (35–55 Ma; Alley et al., 1996) . In situ nucleogenic $^{21}$Ne in our samples is 4%–12% of the excess $^{21}$Ne (Table 1).

Crustal nucleogenic $^{21}$Ne is produced mainly by the reactions $^{24}Mg(n, \alpha)^{21}Ne$ and $^{18}O(\alpha, n)^{21}Ne$, and probably accumulates in crustal fluids, subsequently incorporated in quartz (or silcrete) during crystallization. Estimated crustal nucleogenic $^{21}$Ne is based on the amounts of crustal radiogenic $^{40}$Ar and fissiogenic $^{136}$Xe (produced from decay

TABLE 1. RESULTS OF NOBLE GAS, U, Th, AND K ANALYSES AND INTERFERENCE CORRECTIONS IN SILCRETE GIBBER SAMPLES

| | G115 | G199 | G499 |
|---|---|---|---|
| [$^{20}$Ne] | 6.33 | 5.40 | 6.04 |
| ($10^{-9}$cm$^3$STP g$^{-1}$) | ±0.16 | ±0.13 | ±0.15 |
| $^{21}$Ne/$^{20}$Ne | 3.53 | 3.65 | 3.80 |
| ($10^{-3}$) | ±0.02 | ±0.02 | ±0.02 |
| $^{22}$Ne/$^{20}$Ne | 10.16 | 10.35 | 10.17 |
| ($10^{-2}$) | ±0.03 | ±0.03 | ±0.03 |
| Excess $^{21}$Ne | 3.63 | 3.75 | 5.05 |
| ($10^{-12}$cm$^3$STP g$^{-1}$) | ±0.13 | ±0.13 | ±0.16 |
| [$^{36}$Ar] | 5.32 | 6.06 | 11.39 |
| ($10^{-9}$cm$^3$STP g$^{-1}$) | ±0.10 | ±0.11 | ±0.21 |
| $^{40}$Ar/$^{36}$Ar | 379 | 872 | 692 |
| | ±1 | ±2 | ±1 |
| [$^{130}$Xe] | 0.578 | 0.678 | 1.33 |
| ($10^{-12}$cm$^3$STP g$^{-1}$) | ±0.038 | ±0.044 | ±0.09 |
| $^{136}$Xe/$^{130}$Xe | 2.40 | 2.36 | 2.24 |
| | ±0.02 | ±0.02 | ±0.02 |
| U | 0.815 | 0.449 | 0.335 |
| (ppm) | ±0.058 | ±0.042 | ±0.023 |
| Th | 2.03 | 1.36 | 0.85 |
| (ppm) | ±0.13 | ±0.11 | ±0.06 |
| K | N.D.* | 146 | 98 |
| (ppm) | | ±7 | ±1 |
| Fractions in excess $^{21}$Ne (%) | | | |
| In situ nucleogenic | 11.9 | 7.0 | 3.6 |
| Crustal nucleogenic | 0.2 | 9.5 | 16.0 |
| Cosmogenic | 87.8 | 83.5 | 80.4 |

*Note*: Noble gases were extracted by total fusion at 1800°C, and analyzed by VG5400 noble gas mass spectrometer (Honda et al., 1993). U and Th, and K were analyzed by ICP-MS, and Flame Photometer, respectively. The amounts of cosmogenic $^{21}$Ne in the samples were determined by subtracting in situ and crustal nucleogenic $^{21}$Ne from excess $^{21}$Ne (see text).

*N.D. = not determined.

TABLE 2. COSMOGENIC NUCLIDE DATA AND EXPOSURE AGES

| | G115 | G199 | G499 |
|---|---|---|---|
| Latitude (°S) | 28.6 | 27.2 | 27.2 |
| Altitude (m) | 250 | 220 | 250 |
| $^{21}$Ne* | 84.0 | 84.5 | 107.0 |
| ($10^6$ atoms g$^{-1}$) | ±3.5 | ±3.9 | ±9.8 |
| $^{10}$Be* | 9.59 | 6.63 | 8.29 |
| ($10^6$ atoms g$^{-1}$) | ±0.47 | ±0.31 | ±0.31 |
| Apparent exposure age (Ma) | | | |
| $^{21}$Ne | 4.1 | 4.2 | 5.3 |
| | ±0.8 | ±0.9 | ±1.2 |
| $^{10}$Be | 4.3 | 2.0 | 3.0 |
| | ±0.5 | ±0.4 | ±0.4 |
| Model exposure age† | N.A.§ | 1.86 | 2.86 |
| (Ma) | | ±0.16 | ±0.26 |

*Normalized to sea level and high latitude using Lal's (1991) scaling method.
†Calculated with $^{21}$Ne and $^{10}$Be production rates [at sea level, high latitude (>60°)] = 20.3 and 5.1 atoms g$^{-1}$, respectively (Niedermann, 2000; Stone, 2000), $^{10}$Be decay constant = $4.59 \times 10^{-7}$ yr$^{-1}$, $\rho = 2.65$ g cm$^{-3}$ and $\Lambda = 160$ g cm$^{-2}$
§N.A. = not applicable.

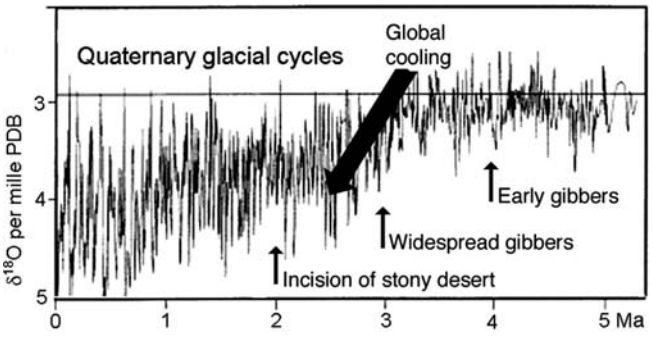


**Figure 3. Gibber ages (arrows) indicate that Australia's stony deserts formed during late Cenozoic global cooling as seen in marine sediments (benthic oxygen isotopes: east Atlantic Ocean Drilling Program Site 659; Tiedemann et al., 1994), that led to Quaternary glacial cycles and heightened aridity (loess formation; Ding et al., 2002) in northwest China. PDB—Peedee belemnite.**

of $^{40}$K and spontaneous fission of $^{238}$U, respectively). Before crustal radiogenic $^{40}$Ar and fissiogenic $^{136}$Xe are estimated, in situ radiogenic $^{40}$Ar and fissiogenic $^{136}$Xe are calculated from K and U contents (Table 1) plus the silcrete formation age, and are subtracted from the total nonatmospheric $^{40}$Ar and $^{136}$Xe. For our samples, in situ radiogenic $^{40}$Ar is <6% of the excess $^{40}$Ar, while in situ fissiogenic $^{136}$Xe is 13%–22% of the excess $^{136}$Xe. Crustal nucleogenic $^{21}$Ne is estimated from the amounts of crustal radiogenic $^{40}$Ar and fissiogenic $^{136}$Xe, using known production ratios in the average crust (nucleogenic $^{21}$Ne/fissiogenic $^{136}$Xe = 15, radiogenic $^{40}$Ar/fissiogenic $^{136}$Xe = $7.3 \times 10^7$ with Th/U = 3 and K/U = 12,000; Honda et al., 2004). Crustal nucleogenic $^{21}$Ne is 0.2%–16% of excess $^{21}$Ne in our samples; total nucleogenic $^{21}$Ne is 12%–20%, and cosmogenic $^{21}$Ne is 80%–88% of the excess (Table 1).

## RESULTS AND DISCUSSION

Exposure ages were calculated for $^{10}$Be and $^{21}$Ne. Lal (1991) showed that cosmogenic nuclide N content (atoms per gram) in rock at the ground surface depends on the erosion rate $\boldsymbol{\varepsilon}$ and exposure age $t$

$$N = P_0\{1 - \exp[-(\lambda + \mu\boldsymbol{\varepsilon})t]\}/(\lambda + \mu\boldsymbol{\varepsilon}) + N_0\exp(-\lambda t), \quad (1)$$

where $P_0$ is ground-surface production rate of the nuclide at the site latitude and altitude, and $\lambda$ is radioactive decay constant of the nuclide. The absorption coefficient $\mu = \rho/\Lambda$; $\rho$ is density of the medium and $\Lambda$ is absorption mean free path of cosmic-ray nucleons. $N_0$ represents any initial amount of the nuclide that accumulated before exposure. Conventionally, $N_0$ is assumed to be zero and the first RHS term in equation 1 is used to calculate exposure ages by assuming $\boldsymbol{\varepsilon} = 0$, or erosion rates by assuming that $\varepsilon$ is constant and $t \gg 1/(\lambda + \mu\boldsymbol{\varepsilon})$. Table 2 shows conventional (or apparent) exposure ages calculated for $^{10}$Be and $^{21}$Ne, with $N_0$ and $\boldsymbol{\varepsilon}$ set to zero, and recent determinations of nuclide production rates (Niedermann, 2000; Stone, 2000). Apparent exposure ages (Table 2) range from 2.0 to 5.3 Ma. $^{21}$Ne and $^{10}$Be ages for sample G115 are very similar, but $^{21}$Ne ages for G199 and G499 exceed their $^{10}$Be ages.

The difference between $^{21}$Ne and $^{10}$Be ages is significant, and implies that cosmogenic $^{21}$Ne had accumulated before the parent silcrete was exposed at the ground surface. Cosmogenic production can occur to >10 m depth below the surface: spallation reactions dominate near the surface ($\Lambda \sim 160$ g cm$^{-2}$), but muon-capture reactions, which contribute only ~3% of production at the surface, dominate at greater depths ($\Lambda \sim 1300$ g cm$^{-2}$) (Brown et al., 1995; Lal, 1991). Preexposure production at a shallow depth $h$ for an interval $t_0$ would produce both $^{21}$Ne and $^{10}$Be. When $t_0 \gg 1/\lambda_{Be}$, $N_0^{Be}$ becomes constant, but $N_0^{Ne}$ can only increase with time and the conventional $^{21}$Ne age of a sample thus becomes greater than its $^{10}$Be age.

Because the apparent $^{21}$Ne and $^{10}$Be ages for G199 and G499 are significantly discordant, indicating that the silcrete was at a shallow depth before being stripped and exposed, we recalculated exposure ages using paired $^{21}$Ne-$^{10}$Be data, assuming that the parent silcrete was formed 45 Ma and was buried at average depth $h$ until it was exhumed. With this model, G199 and G499 gave postexposure ages of 1.86 ± 0.16 and 2.86 ± 0.26 Ma, respectively, with preexposure mean depth $h \sim 2.0$ m (Table 2). (We note that preexposure cover depths almost certainly varied through time, and model $h$ values represent weighted mean depths.) The assumed age of silcrete formation has little effect on these estimates: for a silcrete age of 35 Ma the exposure ages are only ~2% younger, and preexposure depths are ~12% less. Finally, to allow for possible erosion of the gibbers, we also calculated postexposure ages with an erosion rate $\boldsymbol{\varepsilon} = 5$ cm m.y.$^{-1}$ (this is a likely maximum: 20–30 cm silcrete clasts would reduce to centimeter size gibbers in 2–3 m.y.): resultant ages are as much as 30% older than the no-erosion case. No comparable calculation was done for sample G115 (site B) because it gave accordant $^{21}$Ne and $^{10}$Be ages (Table 2), implying that the parent silcrete in this case was significantly deeper than a few meters before it was exhumed.

## CONCLUSIONS

Using in situ cosmogenic $^{10}$Be and $^{21}$Ne in silcrete gibbers, we estimate that stripping of soil mantles from silcrete tableland in southern central Australia began ca. 4 Ma. Following exposure of underlying silcrete, stony desert was actively forming 3 Ma. The depth of soil stripped from the parent silcrete varies: <2.5 m was lost in area A but significantly more was stripped from the source of the gibbers at site B. Dissection of the tableland, probably initiated earlier by broad tectonic warping, continued during the development of stony desert. The presence of gibbers with postexposure ages of ca. 2 Ma on a fan surface <1 km from their valley-head sources suggests that dissection of the silcrete tableland has slowed in the past 2 m.y. Once formed, stony desert persists: the gibber pavement inhibits soil regeneration and increases runoff.

Australia's northward drift positioned it in latitudes that are dry today, and enhanced the sensitivity of its landscape to climatic drying. Our exposure-age results show that Australia's stony desert formed and aridity deepened at a time of global cooling that initiated the Quaternary ice ages and increased aridity elsewhere, notably north China (Fig. 3). The number of measured samples is small, but these successful

measurements of $^{21}$Ne-$^{10}$Be demonstrate the advantages of a radioactive/stable pair of nuclides for determining landscape history.

**ACKNOWLEDGMENTS**

We thank the reviewers for their careful review and constructive comments. We are pleased to acknowledge support for this research from the Australian Research Council grant DP0342689, and thank A. Heimsath for collaboration.

**REFERENCES CITED**

Alley, N.F., Krieg, G.W., and Callen, R.A., 1996, Early Tertiary Eyre Formation, lower Nelly Creek, southern Lake Eyre Basin, Australia: Palynological dating of macrofloras and silcrete, and palaeoclimatic interpretations: Australian Journal of Earth Sciences, v. 43, p. 71–84.

Benbow, M.C., Alley, N.F., Callen, R.A., and Greenwood, D.R., 1995a, Geological history and palaeoclimate, *in* Drexel, J.F., and Preiss, W.V., eds., The geology of South Australia, Volume 2: The Phanerozoic: South Australia Geological Survey Bulletin 54, p. 208–217.

Benbow, M.C., Callen, R.A., Bourman, R.P., and Alley, N.F., 1995b, Deep weathering, ferricrete and silcrete, *in* Drexel, J.F., and Preiss, W.V., eds., The geology of South Australia, Volume 2: The Phanerozoic: South Australia Geological Survey Bulletin 54, p. 201–207.

Bowler, J.M., 1982, Aridity in the late Tertiary and Quaternary of Australia, *in* Barker, W.R., and Greenslade, P.J.M., eds., Evolution of the flora and fauna of arid Australia: Norwood, South Australia, Peacock Publications, p. 35–45.

Brown, E.T., Bourlès, D.L., Colin, F., Raisbeck, G.M., Yiou, F., and Desgarceaux, S., 1995, Evidence for muon-induced production of $^{10}$Be in near-surface rocks from the Congo: Geophysical Research Letters, v. 22, p. 703–706, doi: 10.1029/95GL00167.

Callen, R.A., and Benbow, M.C., 1995, The deserts—Playas, dunefields and watercourses, *in* Drexel, J.F., and Preiss, W.V., eds., The geology of South Australia, Volume 2: The Phanerozoic: South Australia Geological Survey Bulletin 54, p. 244–251.

Cook, E.R., Woodhouse, C.A., Eakin, C.M., Meko, D.M., and Stahle, D.W., 2004, Long-term aridity changes in the western United States: Science, v. 306, p. 1015–1018, doi: 10.1126/science.1102586.

Ding, Z.L., Derbyshire, E., Yang, S.L., Yu, Z.W., Xiong, S.F., and Liu, T.S., 2002, Stacked 2.6-Ma grain size record from the Chinese loess based on five sections and correlation with the deep-sea $\delta^{18}$O record: Paleoceanography, v. 17, p. 21.

English, P., Spooner, N.A., Chappell, J., Questiaux, D.G., and Hill, N.G., 2001, Lake Lewis basin, central Australia: Environmental evolution and OSL chronology: Quaternary International, v. 83–85, p. 81–101, doi: 10.1016/S1040-6182(01)00032-5.

Fifield, L.K., 1999, Accelerator mass spectrometry and its applications: Reports on Progress in Physics, v. 62, p. 1223–1274, doi: 10.1088/0034-4885/62/8/202.

Gosse, J.C., and Phillips, F.M., 2001, Terrestrial in situ cosmogenic nuclides: Theory and application: Quaternary Science Reviews, v. 20, p. 1475–1560, doi: 10.1016/S0277-3791(00)00171-2.

Hesse, P.P., 1994, The record of continental dust from Australia in Tasman sea sediments: Quaternary Science Reviews, v. 13, p. 257–272, doi: 10.1016/0277-3791(94)90029-9.

Hetzel, R., Niedermann, S., Ivy-Ochs, S., Kubik, P.W., Tao, M., and Gao, B., 2002, $^{21}$Ne versus $^{10}$Be and $^{26}$Al exposure ages of fluvial terraces: The influence of crustal Ne in quartz: Earth and Planetary Science Letters, v. 201, p. 575–591, doi: 10.1016/S0012-821X(02)00748-3.

Hill, R.S., ed., 1994, The history of Australian vegetation: Cretaceous to recent: Cambridge, UK, Cambridge University Press, 433 p.

Honda, M., McDougall, I., Patterson, D.B., Doulgeris, A., and Clague, D.A., 1993, Noble gases in submarine pillow basalt glasses from Loihi and Kilauea, Hawaii: A solar component in the Earth: Geochimica et Cosmochimica Acta, v. 57, p. 859–874, doi: 10.1016/0016-7037(93)90174-U.

Honda, M., Phillips, D., Harris, J.W., and Yatsevich, I., 2004, Unusual noble gas compositions in polycrystalline diamonds: Preliminary results from the Jwaneng kimberlite, Botswana: Chemical Geology, v. 203, p. 347–358, doi: 10.1016/j.chemgeo.2003.10.012.

Kennedy, B.M., Hiyagon, H., and Reynolds, J.H., 1990, Crustal neon: A striking uniformity: Earth and Planetary Science Letters, v. 98, p. 277–286, doi: 10.1016/0012-821X(90)90030-2.

Kohl, C.P., and Nishiizumi, K., 1992, Chemical isolation of quartz for measurements of in-situ-produced cosmogenic nuclides: Geochimica et Cosmochimica Acta, v. 56, p. 3583–3587, doi: 10.1016/0016-7037(92)90401-4.

Lal, D., 1991, Cosmic ray labeling of erosion surfaces: In situ nuclide production rates and erosion models: Earth and Planetary Science Letters, v. 104, p. 424–439, doi: 10.1016/0012-821X(91)90220-C.

Mabbutt, J.A., 1977, An introduction to systematic geomorphology, 2: Desert landforms: Canberra, Australian National University Press, 340 p.

Nanson, G.C., Chen, X.Y., and Price, D.M., 1995, Aeolian and fluvial evidence of changing climate and wind patterns during the past 100 ka in the western Simpson Desert, Australia: Palaeogeography, Palaeoclimatology, Palaeoecology, v. 113, p. 87–102, doi: 10.1016/0031-0182(95)00064-S.

Niedermann, S., 2000, The $^{21}$Ne production rate in quartz revisited: Earth and Planetary Science Letters, v. 183, p. 361–364, doi: 10.1016/S0012-821X(00)00302-2.

Niedermann, S., Graf, T., Kim, J.S., Kohl, C.P., Marti, K., and Nishiizumi, K., 1994, Cosmic-ray-produced $^{21}$Ne in terrestrial quartz: The neon inventory of Sierra Nevada quartz separates: Earth and Planetary Science Letters, v. 125, p. 341–355, doi: 10.1016/0012-821X(94)90225-9.

Simon-Coicon, R., Milnes, A.R., Thiry, M., and Wright, M.J., 1996, Evolution of landscapes in northern South Australia in relation to the distribution and formation of silcretes: Geological Society [London] Journal, v. 153, p. 467–480.

Stone, J.O., 2000, Air pressure and cosmogenic isotope production: Journal of Geophysical Research, v. 105, p. 23,753–23,759, doi: 10.1029/2000JB900181.

Thiry, M., and Milnes, A.R., 1991, Pedogenic and groundwater silcrete at Stuart Creek opal field, South Australia: Journal of Sedimentary Geology, v. 61, p. 111–127.

Tiedemann, R., Sarnthein, M., and Shackleton, N.J., 1994, Astronomic timescale for the Pliocene Atlantic $\delta^{18}$O and dust flux records of Ocean Drilling Program Site 659: Paleoceanography, v. 9, p. 619–638, doi: 10.1029/94PA00208.

Wasson, R.J., 1983, The Cainozoic history of the Strzelecki and Simpson dunefields (Australia) and the origin of the desert dunes: Zeitschrift für Geomorphologie, v. 45, p. 85–115.

White, M.E., 1994, After the greening, the browning of Australia: Kenthurst, Australia, Kangaroo Press, 288 p.

Yatsevich, I., and Honda, M., 1997, Production of nucleogenic neon in the Earth from natural radioactive decay: Journal of Geophysical Research, v. 102, p. 10,291–10,298, doi: 10.1029/97JB00395.

Manuscript received 28 March 2005
Revised manuscript received 24 August 2005
Manuscript accepted 27 August 2005

Printed in USA